PNEUMATICALLY ACTUATED BIOMIMETIC PARTICLE TRANSPORTER

A. Rockenbach[1], Chr. Brücker[2], and U. Schnakenberg[1]
[1]Insitute of Materials in Electrical Engineering 1, RWTH Aachen University, Germany
[2]Institute for Mechanics and Fluid Dynamics, TU Bergakademie Freiberg, Freiberg, Germany

ABSTRACT

To prevent the adhesion of particles at surfaces by transporting them along the surface a new type of pneumatically actuated particle transporter is introduced. The biomimetic approach is based on the transportation principle of particles by cilia arrays due to the generation of metachronal waves. Rows of flaps, which mimic the cilia, are asymmetrically positioned on flexible membranes. The membranes are individually deflected by applying a well-defined pressure profile to achieve a metachronal wave.

Detailed simulations of the membrane and flap deflections as well as a description of the proof-of-concept by applying metachronal waves to the flap arrays are presented.

INTRODUCTION

In microfluidic devices, a couple of methods to transport and separate particles in closed channels exist, like electrophoresis, electromagnetism, physicochemical transport, or peristalsis. In some cases, however, particle transport in open channels is required (absence of a second wall). Here the traditional transport mechanisms are not applicable due to the absence of a second border.

The transportation of the fluid along the surface can be achieved by using cilia like structures to push the fluid along the surface by generation of metachronal waves. In nature many ciliated surfaces are known, such as the respiratory tract [1] or the fallopian tube [2]. In addition, the use of cilia as propelling mechanism for bacteria [3] or Ctenophore are known and well-studied also in numerical analysis [4,5].

First studies to mimic cilia-type actuation using magnetic actuation principle were published in [6,7], whereas an oscillating force principle at the free end of the artificial cilia was investigated in [8].

The objective is the development of particle transportation near a surface by a biomimetic adaptation of a cilia principle. Here, the actuation of the artificial cilia array is carried out by using a micro pneumatic excitation.

DESIGN CONCEPT

The basic concept of the particle transporter chip is shown in Figure 1. Rows of cilia-like flaps are positioned asymmetrically on bendable membranes. Each flap row can be deflected separately by an induced pneumatic force which bends the supporting membrane. The membrane movement converts to large deflections of the flaps in x-direction (lateral) and in smaller movements in z-direction (vertical). Due to the high aspect ratio of the flaps the angle rotation results in a fluid movement parallel to the surface which prevents the particle deposition.

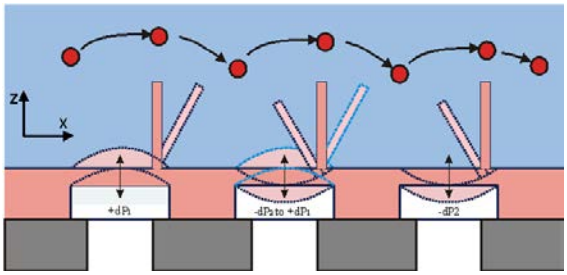

Figure 1: Concept of the pneumatically-actuated particle transporter (cross-section, not in scale): rows of flaps are asymmetrically located on flexible membranes supports. The pressures to deflect the membranes individually are applied to the underlying channels.

Membrane bending is achieved by changing the pressure in the underlying channel from a negative differential pressure to a positive one. The bending cycle must be exactly coordinated to ensure a metachronal wave for an accurate particle transport. The phase difference of pressure in adjacent channels is one of the most important parameters for the transport mechanism.

SIMULATIONS

Simulations were carried out using ANSYS 12 Structural program in two-way coupling with CFX program. Both models were connected to ANSYS internal Fluid-Solid-Interaction (FSI) module. The simulations were based on a 2D model with not linear material. The material data for water was taken from the ANSYS Material Database. PDMS (PolyDiMethylSiloxane), which serves as suitable material for the membrane and flaps, was defined as an isotropic material model. The material parameters were generated by tensile testing [9]. Optimum membrane bending conditions, shown in Figure 2, were extracted for a 600 µm wide and 100 µm thick PDMS membrane. The supporting structure between two membranes was optimized to 400 µm. The optimum flap position on the membrane was determined between 75 µm and 100 µm adjacent from the supporting structure.

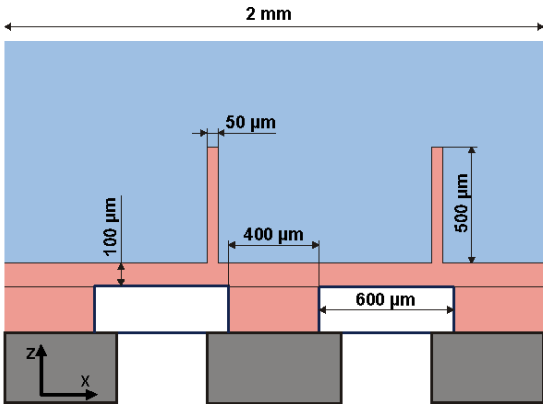

Figure 2: Design details of the particle transporter: the pressure channel under the 100 µm thick membrane is 600 µm wide. In combination with the 400 µm wide supporting structure between two channels a pitch of 1000 µm is defined. The flaps are 500 µm high, 50 µm wide, and 1000 µm long.

The van Mieses stress distribution of the PDMS membrane is shown in Figure 3, when the membrane is deflected under a negative pressure of 30 kPa. With respect to the soft membrane material, the bending deforms the membrane shape and increases the membrane area. This deformations appear in both bending directions of the membrane and are responsible for a shift of the tips deflection.

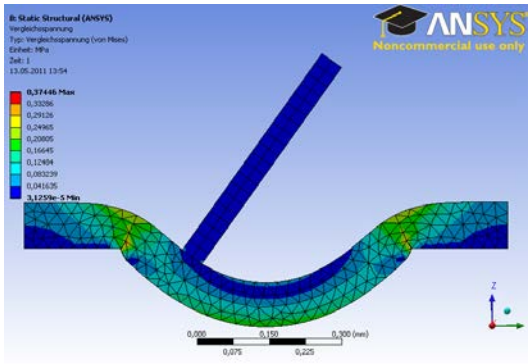

Figure 3: ANSYS 12 FEM simulation of van Mieses stress distribution of a 100 µm thick PDMS membrane deflected by a negative pressure of 30 kPa.

To enhance the pumping effect, the upward bending pressure must have a higher pressure difference from ambient than the downward bending pressure. This leads to a faster flap movement during the upward bending of the membranes.

The asymmetric flap position on the membrane results in an asymmetrical movement of the flap. Figure 5 shows the simulated movement of the flap by setting a minimum and maximum pressure difference of 40 kPa and -30 kPa compared to ambient pressure. The flap moves 480 µm in x-direction and 75 µm in z-direction. This behavior generates a lateral movement in the fluid. A similar characteristic movement was published by Khaderi et al. [10].

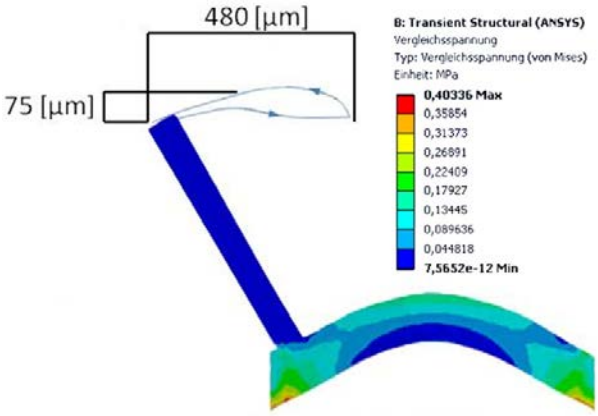

Figure 4: FEM simulation of the flap movement during a forward and backward displacement of the deflected membrane. The blue line represents the movement of the flaps tip during a whole membrane bending cycle, where the applied pressure under the membrane was set to a difference of -30 kPa and +40 kPa compared to ambient pressure. The horizontal displacement was determined to 480 µm, the lateral displacement to 75 µm, respectively. In addition, the van Misis stress distribution in the membrane is shown.

To verify the simulation a simple displacement experiment was carried out. By bending the membrane, with positive or negative differential pressure, in one or the other direction and comparing that to the movement of the tip in the simulation, we proved the simulation results for correctness (Fig. 5).

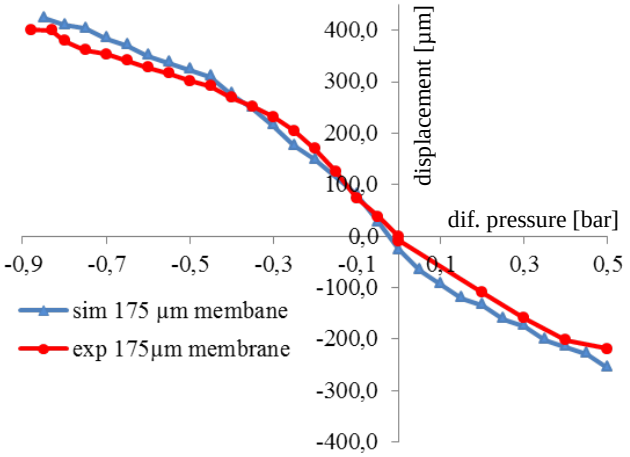

Figure 5: Comparison between simulation(green) and experimental(violet) results of a bended 175 µm thick Sylgard 184(PDMS) membrane, with a 500 µm long flap positioned as shown in Fig. 3. Displacement, in this case, is the movement of the flaps tip away from its rest position.

Figure 6 shows two different, but characteristic streamline profiles. Particles in the fluid follow the circular streamlines whereas particles in vicinity to the flaps are transport-

ed by a net flow. 1000 µm above the membrane surface the flow stops almost completely. For larger distances to the surface no particle transport occurs.

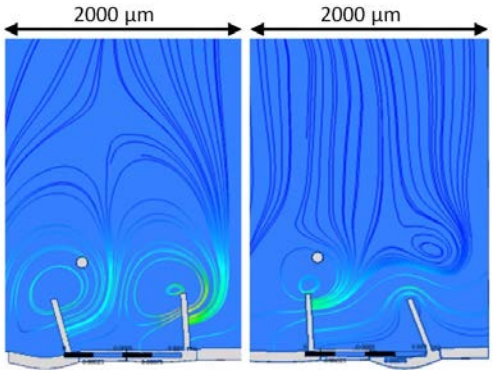

Figure 6: Two different, but characteristic streamline profiles resulting from the FSI-simulations. The membranes are shown at the bottom of the figure. Two bending arrangements are depicted. Above the flaps a particle is shown. The colored lines are streamlines of the fluid. The flow slows down rapidly above the flap. Left: Two rotating flows at the flaps tip. Right: One rotating flow and one laminar streamline profile.

Depending on the dynamic streamline characteristics of the fluid particles follow a net movement, which is shown in Figure 7 where two particle positions are compared. The left green particle corresponds to the start position and the right red particle to the position of the same particle after two membrane bending cycles, respectively, corresponding to a net movement of the particle of 40 µm. This value is about 6% of the amplitude of the tip movement of the flaps.

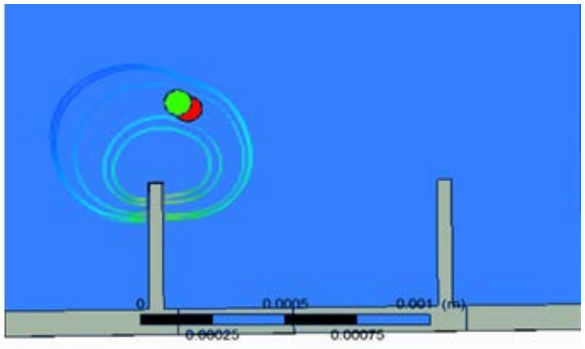

Figure 7: Displacement of a particle (100 µm in diameter) after two membrane bending cycles. The left green particle corresponds to the start position and the right red particle to the end position after two complete load cycles. The distance between the two positions is about 40 µm. The colored lines are streamlines of a specific time step.

Based on these promising results FEM simulations were carried out to generate a metachronal wave by combination the dynamic bending behavior of 8 membranes. The membranes are individually deflected by applying a well-defined pressure profile (from -30 kPa in 50 ms to a pressure of +40 kPa for duration of 50 ms, then again down to -30 kPa in 100 ms) in combination with a defined phase-shift 50 ms between adjacent channels to achieve a metachronal wave, which is necessary for a controlled particle transport [10]. One characteristic simulation result of membrane bending and flap deflection is shown in Figure 8. The stream lines are omitted, because of clarity.

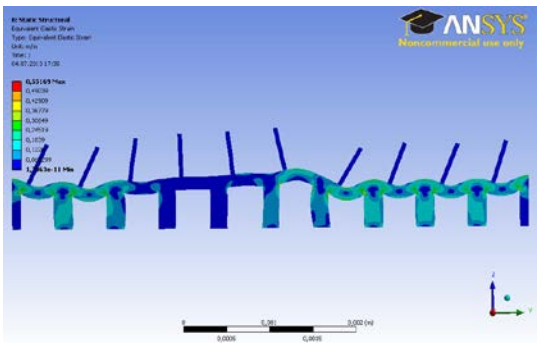

Figure 8: FEM-results of membrane and corresponding flap deflections for establishing a metachronal wave.

FABRICATION

The biomimetic particle transporter chips were fabricated in PMDS using standard soft-lithography techniques in combination with SU-8 micro molds. First, a glass-wafer is coated with chromium by Physical-Vapor-Deposition (PVD). The chromium layer is used to etch a lithography mask right on top of the glass. The structured chromium mask is coated with several layers of SU-8, to reach the desired thickness of 500 µm. Now, to expose the resist, the Wafer is turned around and inserted into the mask aligner. To prevent the SU-8 layer from damage a not reflective material is placed between SU-8 and chuck. The integrated chromium mask structures the resist during exposure. The backside exposure is needed because of high aspect ratio and the negative tone resist profile, which may close the channel or at least makes it difficult to deform the PDMS flaps.

After an adapted Post Exposure Bake (PEB) the wafer is coated with SU-8, again, to realize a second layer on top of the 500 µm thick SU-8 layer. This layer guaranties an optimized positioning of flaps and membrane. In combination with the second mold for the other side of the membrane, it forms a self-assemble structure. The last layer is exposed and aligned from the top.

Figure 9 shows the realized flap array. In the photograph black and grey colored membranes are arranged in 20 rows. On top of each membrane 20 violet colored transparent flaps with a width of 900 µm are arranged in a line. The light grey area is the supporting structure between the channels.

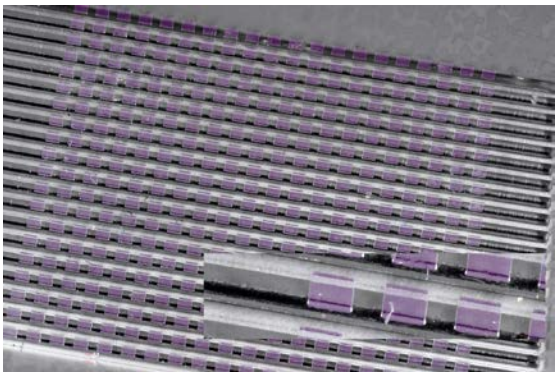

Figure 9: Photograph of the particle transporter chip. 20 membranes (black) are arranged in rows. On each membrane 20 flaps (violet) are realized. The image magnification in the right bottom corner shows three PDMS-based transparent flaps on one membrane over one channel. The gray areas show the supporting structures for the membrane. Scale bar: One flap is 1000 µm wide. The overall dimension of the chip is 3200 µm x 3200 µm.

A detail of the realized flap array is shown in Figure 10. Looking to the top of the chip two membranes arranged vertically is shown. Rows of flaps are arranged asymmetrically on the membrane.

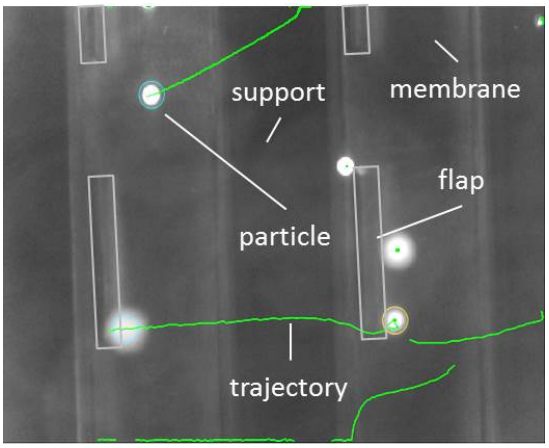

Figure 10: Photograph of a detail of membrane and flap arrangement. On the vertically arranged membranes flaps are arranged vertically. In addition, fluorescence-marked 60 µm polystyrene particles and their corresponding tracked path are shown. Scale bar: The flap is 50 µm 50 µm wide and 1000 µm long.

RESULTS

The particle transporter chip was connected to the pneumatic triggering module and integrated into a microfluidic chamber. A glycol-water mixture of 3:10 was used as fluid to ensure levitating particles. Fluorescence-marked 60 µm polystyrene particles were used. Figure 10 shows a snap-shot of the proof-of-concept (stroboscopic picture for not-deflected flap). Several particles are shown in the flap array. The different diameters correspond to the different vertical positions the particles have with respect to the focus depth of the objective lens (focus is on top of the flap). The trajectories of some particles are shown in green. The particle transportation direction for the given pressure profile to realize a metachronal wave was from the left to the right and the net transport velocity was determined to 30 µm/s.

CONCLUSIONS

A new concept for active particle transport in single interface fluids is introduced. The active movement of cilia-like flaps induce a fluid flow. The flaps are actuated by an interface membrane, bent through pneumatic pressure from the backside. Simulations are carried out to determine an optimized design: Best membrane bending conditions are found for a PDMS membrane with width of 600 µm and a wall width of 400 µm by setting the membrane thickness to 100 µm. An optimum flap position on the membrane is determined between 75 µm and 100 µm from the attachment. The asymmetric position of the flaps on the membrane results in an asymmetric movement of the flaps. The whole horizontal distance of the flap movement is about 480 µm and the vertical movement about 75 µm using a 500 µm high and 50 µm wide flap, respectively. The simulations show that dispersed particles in the fluid will be transported by the flow. They will move almost circular, but the net particle transport will be unidirectional.

ACKNOWLEDGEMENTS

Funding is given by the German Federal Ministry of Education and Research under grant #16SV5341 (PaTra). We gratefully acknowledge the cooperation with our project partners P. Uhlmann, A. Rollberg, and M. Kunder from Leibniz Institute of Polymer Research Dresden e.V. - Dept. Physical Chemistry und Polymer Physics, Dresden, Germany.

REFERENCES

[1] M.A. Sleigh et al., *Am. Rev. of Respir. Dis*, 137 (3) (1988), 726.
[2] R.A. Lyons et al., *Human Reproduction Update*, 12 (4) (2006), 363.
[3] B. Behkam et al., *Appl. Phys. Lett*, 90 (2) (2007), 023902.
[4] A. Dauptain et al., *J Fluids Structures*, 24 (8) (2008), 1156.
[5] A. Vilfan et al., *Phys. Rev. Lett*, 96 (5) (2006), 058102.
[6] S.N. Khaderi et al., *Lab on A Chip*, 11 (12) (2011), 2002.
[7] F. Fahrni et al., *Lab on A Chip*, 9 (23) (2009), 3413.
[8] A. Alexeev et al., *Langmuir*, 24 (21) (2008), 12102.
[9] I. Klamme et al., *Tech. Dig. IEEE MEMS 2008*, (2008), pp.626-629.
[10] J. Elgeti et al., PNAS 110 (12) (2013), 4470.